

# Measuring Ionospheric Electron Density Using the Plasma Frequency Probe

Mark D. Jensen\* and Kay D. Baker†  
Utah State University, Logan, Utah 84322

During the past decade, the plasma frequency probe (PFP) has evolved into an accurate, proven method of measuring electron density in the ionosphere above about 90 km. The instrument uses an electrically short antenna mounted on a sounding rocket that is immersed in the plasma and notes the frequency where the antenna impedance is large and nonreactive. This frequency is closely related to the plasma frequency, which is a direct function of free electron concentration. The probe uses phase-locked loop technology to follow a changing electron density. Several sections of the plasma frequency probe circuitry are unique, especially the voltage-controlled oscillator that uses both an electronically tuned capacitor and inductor to give the wide tuning range needed for electron density measurements. The results from two recent sounding rocket flights (Thunderstorm II and CRIT II) under vastly different plasma conditions demonstrate the capabilities of the PFP and show the importance of in situ electron density measurements for understanding plasma processes.

## Nomenclature

$B$	= magnitude of the Earth's magnetic field
$e$	= electron charge
$f_B$	= electron gyro frequency, $eB/2\pi m$
$f_H$	= upper-hybrid frequency
$f_N$	= plasma frequency
$f_{VCO}$	= VCO frequency
$K_{ant}$	= antenna phase gain, deg/MHz
$K_{det}$	= phase detector gain, V/deg
$K_{fil}$	= loop filter gain, unitless
$K_{VCO}$	= VCO gain, MHz/V
$m$	= electron mass
$N$	= electron density
$\epsilon_0$	= permittivity of free space
$\nu$	= electron-neutral collision frequency
$\omega_1$	= loop filter pole
$\omega_2$	= loop filter zero

## Introduction

THE understanding of many ionospheric processes and radio communications phenomena requires a knowledge of electron density and its spatial structure. The plasma frequency probe was developed by Utah State University for use aboard rockets and spacecraft to make absolute electron density measurements of the local ionospheric plasma. Since the first plasma frequency probe (PFP) was flown over 20 years ago, the instrument has progressed through numerous sounding rocket launches until it is now accepted as a reliable, accurate method for measuring electron density throughout the E and F regions of the ionosphere. Perhaps the most challenging application to date of the PFP was aboard a rocket launched from Wallops Island, Virginia, in May 1989 (CRIT II) in a test of Alfren's critical ionization velocity hypothesis.<sup>1</sup> The crux of this experiment was to search for an anomalous increase of ionization due to an explosively accelerated barium stream. This series of simultaneous measurements relied solely on the plasma frequency probe to make the important electron density measurement in this artificially disturbed environment. This required a new level of performance from the plasma frequency probe, namely, a faster

sample rate to follow dramatic changes of density expected in the event. A major effort during the past several years has resulted in a plasma frequency probe whose performance has been vastly improved and exceeds the requirements of the CRIT II experiment. This paper describes this instrument and its utilization to measure ionospheric electron density.

## Principle of Operation

Electrons in a plasma have a natural resonant frequency known as the electron plasma frequency, dependent on the plasma density<sup>2</sup>:

$$f_N = \frac{1}{2\pi} \sqrt{\frac{Ne^2}{m\epsilon_0}} \quad (1)$$

The PFP uses this relationship to determine electron density by immersing an electrically short antenna in the plasma and noting the frequency where the antenna reactance is zero. This can be thought of in a circuit sense as a parallel resonance where the free space capacitive reactance of the antenna is canceled by the reflected inductive reactance (inertial lag) of the oscillating electrons. This frequency of zero reactance corresponds to the plasma frequency.<sup>2</sup> Figure 1 shows antenna impedance curves based on the theoretical work of Despain<sup>3</sup> for a plasma frequency of 5.0 MHz and an electron-neutral collision frequency of 1.0 MHz. As can be seen, the frequency where the antenna reactance is zero is somewhat higher than 5.0 MHz. This shift is due to the added effects of electron cyclotron motion in the terrestrial magnetic field. The result-

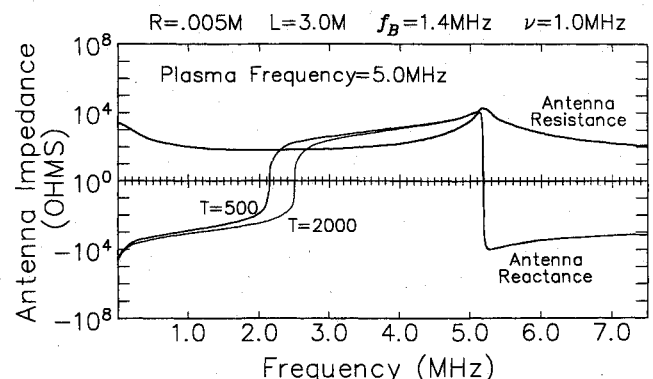


Fig. 1 Impedance curves for cylindrical antenna (Ref. 3).

Received Jan. 14, 1991; revision received Oct. 28, 1991; accepted for publication Oct. 29, 1991. Copyright © 1991 by the American Institute of Aeronautics and Astronautics, Inc. All rights reserved.

\*Research Engineer, Space Dynamics Laboratory.

†Professor, Electrical Engineering and Physics Departments.

ing frequency that gives zero reactance as measured by the PFP is known as the upper-hybrid frequency  $f_H$  and can be expressed as a combination of the plasma frequency  $f_N$  and the electron gyro frequency  $f_B$  (Ref. 2),

$$f_H^2 = f_N^2 + f_B^2 \quad (2)$$

Since to first order the magnitude of the Earth's magnetic field is well known for regions out to an Earth radius or so, the gyro frequency  $f_B$  will also be known. As a result, Eqs. (1) and (2) can be simply solved for electron density:

$$N = \frac{4\pi^2 m \epsilon_0 (f_H^2 - f_B^2)}{e^2} \quad (3)$$

It can be seen from either Eq. (2) or (3) that accurate electron densities are difficult to obtain at low values since the frequency of resonance  $f_H$  will asymptotically approach  $f_B$ . The technique is also limited to regions where a plasma resonance can be observed, i.e., above altitudes where the electron-neutral collisions damp out the resonance. In the natural ionosphere this means the technique will work above about 90 km.

### Instrumentation

The PFP uses a specialized phase-locked loop (PLL) to measure the resonance frequency of the antenna as illustrated in the block diagram of Fig. 2. In the search mode, the voltage-controlled oscillator (VCO) of the PLL starts at its upper frequency limit ( $\approx 20$  MHz) and sweeps to the lower frequency limit ( $\approx 1.2$  MHz) looking for a plasma resonance condition where the antenna reactance is zero. If no resonance is found by the time the VCO reaches its lower frequency limit, then it is reset to the upper limit and the sweep starts over. When a plasma resonance condition is met during a

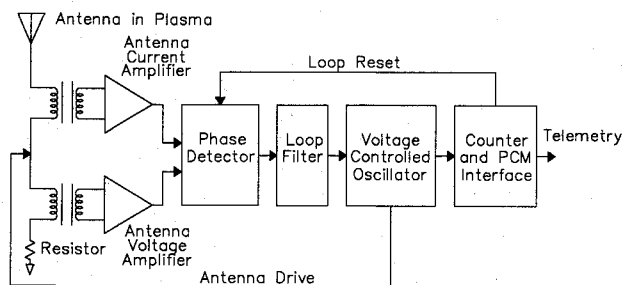


Fig. 2 Plasma frequency probe block diagram.

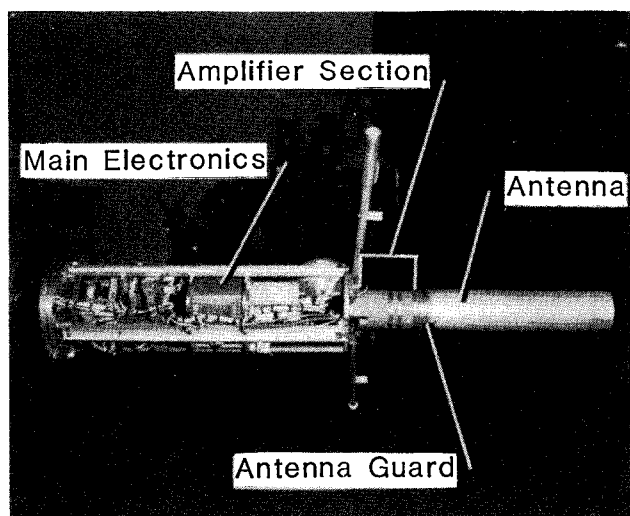


Fig. 3 Forward payload section of NASA Taurus-Nike-Tomahawk 38.007.

sweep, the PLL locks to the frequency of the resonance and tracks the frequency as long as it is within the upper and lower frequency limits of the VCO. The frequency counter then reads an output of this frequency at a typical sample rate of 5 kHz.

Figure 3 is a photograph of one implementation of the PFP in a 9-in. sounding rocket payload (NASA Taurus-Nike-Tomahawk 38.007) that flew successfully in the Thunderstorm II campaign, July 27, 1988. The PFP antenna for this particular payload (Fig. 3) consists of a 5-cm diam cylinder, 20 cm in length, which flies forward just beneath the ejectable nose cone (not shown). The antenna amplifier section fits within the antenna mount. All other electronic sections of the block diagram in Fig. 2 are located within the electronics box labeled as main electronics in Fig. 3. A description of each of these sections follows.

### Antenna and Amplifier

The physical dimensions or placement of the antenna is not critical as long as it is immersed in the plasma and has a large enough free-space capacitance and hence enough rf current to allow the instrument to function properly. All practical antennas will be electrically small at the few MHz frequency ranges of the measurements. In various applications, antennas have been mounted in front or in back of payloads and oriented on or off the rocket spin axis. However, as with any plasma measurement, consideration needs to be given for cases where the antenna may be in the rarified wake region swept out by the fast moving vehicle.

The PFP monitors the phase angle between the antenna voltage and current. When plasma resonance is encountered, the antenna is purely resistive with a large magnitude (see Fig. 1), meaning that the antenna voltage and current are in phase. The PFP uses this zero phase condition between antenna voltage and current to identify a plasma resonance and to lock to it.

The antenna current is monitored through a current transformer that effectively isolates the antenna from the amplifier as shown in Fig. 2. Similarly, the antenna voltage is monitored by measuring the current through a resistor to ground. Phasing of signals between the current and voltage amplifiers must be closely matched or the accuracy of the PFP will be impaired.

### Phase Detector

The antenna voltage and current signals from the amplifiers are converted into digital waveforms in the phase detector. The resulting pulse stream from the phase detector encodes the phase difference of the two signals in the duty cycle. A zero-deg phase difference in the antenna voltage and current signals produces a 50% duty cycle.

### Loop Filter

The pulse stream from the phase detector is integrated by a second-order loop filter to produce the voltage control signal for the VCO. The loop filter has the following transfer function:

$$T(s) = \frac{K_{fil} \omega_1 (s + \omega_2)}{s(s + \omega_1)} \quad (4)$$

### Voltage-Controlled Oscillator

The plasma frequency probe requires a VCO with a high spectral quality sinewave output and a wide tuning range, greater than 14 to 1 for typical applications. Most conventional VCOs with sinewave outputs incorporate an inductor-capacitor (LC) tuning circuit where the output frequency of the oscillator is controlled using a varactor diode. However, the greatest VCO tuning range available using this technique is only about 5 to 1. For this reason, a unique VCO was developed using both a tuneable inductor and tuneable capacitor (varactor diode). The inductor is wound on a ferrite toroid that is made part of the magnetic circuit of a larger electro-

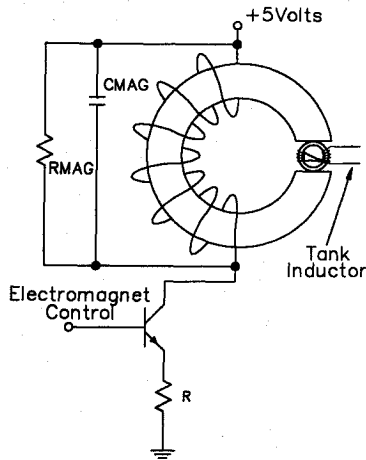


Fig. 4 Inductor tuning circuit for the PFP voltage-controlled oscillator.

magnet as shown in Fig. 4. Varying the current in the windings of the electromagnet increases or decreases the magnetic flux density in the tuning inductor, thereby changing the effective permeability of the ferrite material as it moves up and down on the magnetic flux density-magnetic field (B-H) curve. Since inductance is proportional to the permeability of the core,<sup>4</sup> a changing current in the electromagnet will result in a changing VCO output frequency.

The oscillator is a Motorola MC12061 that was intended for use as a crystal oscillator. The crystal can be replaced, as is the case here, with an equivalent series LC circuit. The MC12061 has the added advantage of having both sinewave (rf) and transistor transistor logic (TTL) outputs, which eases the interface requirements to the antenna and digital counters. More details of the VCO and the unique tuning method can be found in Refs. 5 and 6.

#### Counter and PCM Interface

The output frequency of the VCO is counted for a known period of time or window (approximately 0.16 ms for 5-kHz sampling) and shifted into the pulse coded modulation (PCM) bit stream of the rocket telemetry system. The average frequency for one window can be easily found by dividing the number of counts by the window length. There is a tradeoff here; fast sample rates will result in less accurate frequency counts since fewer numbers of counting bits can be used. The counting window should be as long as possible between PCM sample times to increase the accuracy of the counted frequency and avoid distortion of data for any spectral analysis of electron density fluctuations.<sup>7</sup>

The counter and PCM interface section also provide a reset pulse to the PLL if the output frequency of the VCO ever falls below a set frequency. This reset pulse disables the phase detector, causing the loop to sweep upward to the maximum VCO frequency.

#### Control of the Plasma Frequency Probe

The loop filter acts as an anti-aliasing filter for the PFP. The cutoff frequency of the loop should be set so changes in the signal occurring faster than half the PCM sample rate are filtered out and not aliased into PFP data.<sup>8</sup> Setting the loop cutoff frequency is similar to any standard phase-locked loop and involves choosing the values for the loop filters along with the necessary gain to cause the open-loop transfer function [Eq. (5)] to be equal to unity at the desired cutoff frequency:

$$T(s) = K_{\text{ant}} K_{\text{det}} K_{\text{fil}} K_{\text{VCO}} \omega_1 \frac{(s + \omega_2)}{s(s + \omega_1)} \quad (5)$$

The antenna phase gain can be thought of as relating to the quality factor  $Q$  of the plasma resonance. In other words, for

a small change in frequency near a plasma resonance, how many degrees does the phase angle between the real and imaginary components of the antenna impedance change? Depending on the importance of plasma processes such as electron collisions, propagating waves, and electron temperature, the antenna phase gain can vary, which must be considered when calculating the loop cutoff frequency.

The best performance from the PFP results when the loop filter pole and zero [Eqs. (4) and (5)] are relatively close to each other. If the pole and zero are too far apart, overshoot and ringing in the loop will occur. Not only will the loop have unwanted oscillations around a plasma frequency, but also, if a sudden jump in electron density should occur, the loop could shoot past the plasma resonance, missing it entirely. For optimum response, the loop should be critically damped, although some overshoot can be tolerated, depending on the placement of the pole and zero.

#### Instrument Capabilities

There are five major areas to evaluate the performance of the plasma frequency probe: 1) lowest measurable electron density, 2) accuracy, 3) VCO frequency range, 4) measurement response time to changing density or loop response, and 5) loop reset frequency. The results of the analyses of each of the PFP system attributes are outlined in Table 1. The first item, lowest measurable density, is from the Thunderstorm II sounding rocket campaign and is the lowest density measured by the plasma frequency probe to date.

The accuracy of the instrument can be looked at in two ways. The first is the accuracy of the indicated frequency to the actual resonance frequency. This is evaluated using tuned LC circuits to simulate the upper-hybrid resonance of a plasma. The percent error in frequency as shown in Table 1 is within the error of the calibration techniques of the tuned circuits. The second way to look at instrument errors, shown in Table 1, is through electron density calculations. Equation (3) shows that a difference between squares is taken between the upper-hybrid  $f_H$  and electron gyro frequencies  $f_B$  to calculate the electron density. As a result, taking the difference of two almost equal numbers gives increasingly large errors as the gyro frequency is approached, which can be readily seen in Table 1 for low values of  $f_H$ .

The VCO range shown in Table 1 can be greater than 25 to 1 thanks to the unique tuning method explained in the instrumentation section. For most applications, a 14 to 1 tuning range is adequate; however, because the instrument has the capability of a wider tuning range, special active, artificially disturbed ionosphere experiments such as CRIT II can be supported.

The ability of the PFP to quickly follow changing electron density continues to increase to higher frequencies. In Table 1 the loop response is listed as greater than 10 kHz. To date, the

Table 1 Plasma frequency probe capabilities

Actual $f_H$ , MHz	Measured $f_H$ , MHz	Accuracy	
		% error	Density % error at $f_B = 1.5$ MHz
2.030	2.033	+ 0.15	+ 0.65
4.000	3.993	- 0.18	- 0.41
6.000	6.001	+ 0.02	+ 0.04
8.110	8.118	+ 0.10	+ 0.20
10.000	10.042	+ 0.42	+ 0.86
12.000	12.082	+ 0.68	+ 1.39
Lowest measureable density <sup>a</sup>		$7 \times 10^3$ electrons/cm <sup>3</sup>	
VCO frequency range		500 kHz < $f_{\text{VCO}}$ < 25 MHz	
Loop response		> 10 kHz	
Loop reset frequency <sup>b</sup>		857 Hz	

<sup>a</sup>From Thunderstorm II, July 27, 1988.

<sup>b</sup> $f_{\text{VCO}}$  (low-high-low), at loop cutoff of 6 kHz.

fastest PFP flown was the CRIT II instrument, which was set at a loop response of 6 kHz. The fastest instrument tested on the bench had a loop response of 10 kHz and functioned with no problems. The limiting factor to the loop response is the speed of the VCO. At present, the lowest rate of change for the VCO is 30 kHz.

The last item in Table 1 is the loop reset frequency. This is a measure of how fast the PFP will reset to the highest VCO output frequency and sweep downward to the lowest VCO frequency searching for a plasma resonance. The speed of the reset is coupled to the loop gain. Shown in Table 1 is the reset frequency for the CRIT II instrument.

### In-Flight Performance

As an example of the in-flight performance of the plasma frequency probe, the electron density results from the Thunderstorm II campaign are shown in Fig. 5 in terms of a reduced electron density vs altitude profile for the ascent portion of the rocket flight. The probe initially did not lock onto the local plasma resonance until the density increased to the threshold of the probe at an altitude of about 236 km where the density reached  $7 \times 10^3 \text{ cm}^{-3}$ . The probe then remained locked, giving a continuous measure of the electron density up through apogee of 450 km and down to about the same electron density on rocket descent. The profile shows an F region with a broad peak at about 355 km with a peak electron density of  $1.6 \times 10^5 \text{ cm}^{-3}$ . Above the peak the density falls off slowly with altitude up to 450 km. A lot of spatial structure in the electron density is apparent on the bottom side of the F layer, i.e., below the F-layer peak. Less structure is observed in the topside region above the peak.

This example of plasma frequency probe results is, perhaps, a worst case in terms of the regions where the probe was below its threshold since this rocket flight occurred at night and on a night when the electron density was particularly low well up into the F region of the ionosphere. This illustrates the low density limit of the technique under conditions of low ionospheric electron densities. Over the region that the density exceeded the  $7 \times 10^3 \text{ cm}^{-3}$  lower limit, the probe provided continuous values of electron density.

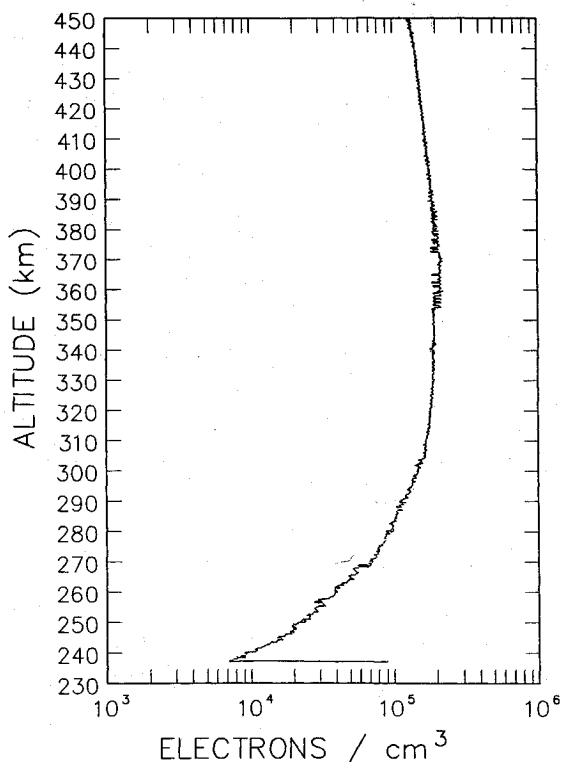


Fig. 5 Electron density profile (ascent) from the Thunderstorm II campaign.

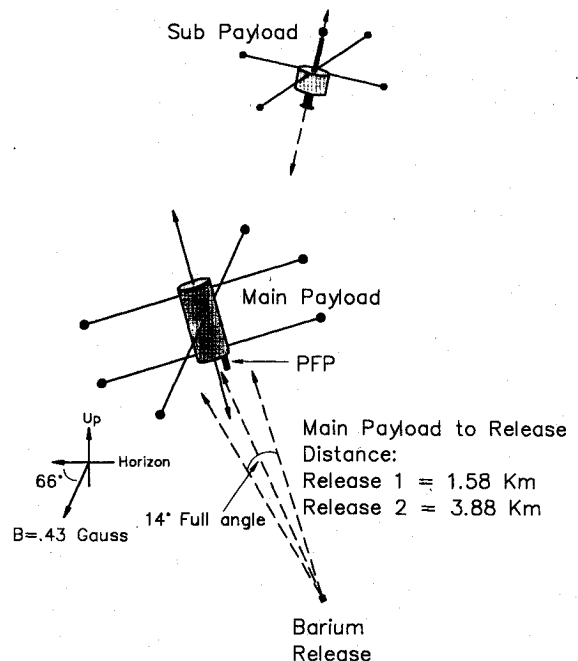
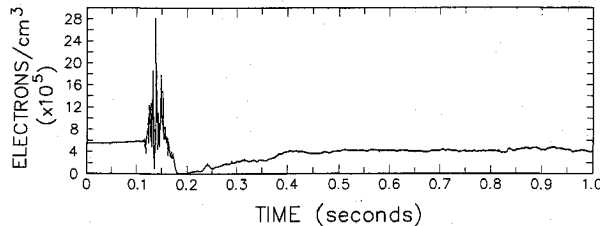


Fig. 6 Simplified CRIT II experiment geometry.

A second illustration of the probe performance and its capabilities to follow fast changing electron densities is the CRIT II experiment where the probe was called upon to provide electron density measurements produced by an explosively propelled burst of barium vapor in a test of Alfvén's critical ionization velocity hypothesis.<sup>1</sup> A simple geometry of this experiment is shown in Fig. 6. For a more detailed explanation of the CRIT II experiment, see Ref. 9. The plasma frequency probe was located at the rear of the main payload, which was at a distance of 1.58 km (Release 1) from the shaped charge that directed the barium vapor toward the main payload. Since the measurement was performed in a very disturbed environment, dc probes would not provide reliable measurements due to the variation in the reference potential of the vehicle. The plasma frequency probe is the only technique that can make the measurement locally in this disturbed environment. The plasma frequency probe results in Fig. 7 show the effects of the barium burst arriving at the main payload. The plot gives the measured electron density vs time in seconds after the barium burst. Up until about 0.1 s after the burst, the electron density observed is that of the undisturbed background F region of  $5.4 \times 10^5 \text{ cm}^{-3}$  at the payload altitude of about 430 km. Shortly thereafter the dramatic increase in ionization due to the arrival of the barium stream can be seen. The density is seen to increase to a maximum of about  $2.8 \times 10^6 \text{ cm}^{-3}$  with extreme structure. The end of the region with increased density, around 0.17 s, corresponds to a velocity of the beam of about 9 km/s. The width of the region of enhanced electron density implies a width along the neutral beam of about 900 m if the observed disturbances are traveling with the beam. The spiky nature of the observed electron density features are notable. The fast response of the probe allows it to follow these dramatic changes. The implications are that either there are bursts of intense ionization or that the ions are bunched together by some mechanism. Intense regions of ionization are followed by regions of depletion of plasma, possibly due to rapid expansions of newly produced hot electrons. Particularly notable is the depletion hole at about 0.138 s where the density drops well below the background density to a value of about  $8 \times 10^4 \text{ cm}^{-3}$ . After about 0.17 s (well after the passage of the ionization front), a large depletion region is observed that persists for over a second. The minimum value of electron density in this hole is below  $10^4 \text{ cm}^{-3}$ .



**Fig. 7 Enhanced electron density due to critical ionization velocity effect, CRIT II experiment.**

Due to the ability of the probe to follow the dramatic changes in electron density resulting from the arrival of the barium stream, verification of the critical ionization velocity has been obtained, and the complex, rapidly varying structure is being studied for what it reveals about the complex plasma phenomena occurring in this active experiment.

### Conclusions

The plasma frequency probe has developed into a very accurate and unique electron density measurement technique. Hours of bench testing and instrument engineering have brought performance to a new level, and numerous sounding rocket flights have proven the PFP as a reliable, valuable instrument in understanding ionospheric plasma processes.

### Acknowledgments

This work was supported under NASA Grant NAG5-603. Special thanks are extended to L. Carl Howlett and Jay C. Ballard of Space Dynamics Laboratory, Utah State Univer-

sity, who did much of the earlier development of the plasma frequency probe and contributed significantly with insight and expertise to recent developments.

### References

- <sup>1</sup>Torbert, R. B., "Critical Velocity Experiments in Space," *Advances in Space Research*, Vol. 8, No. 1, 1988, pp. 39-49.
- <sup>2</sup>Baker, K. D., Despaigne, A. M., and Ulwick, J. C., "Simultaneous Comparison of RF Probe Techniques for Determination of Ionospheric Electron Density," *Journal of Geophysical Research*, Vol. 71, No. 3, 1966, pp. 935-944.
- <sup>3</sup>Despaigne, A. M., "Antenna Impedance in the Ionosphere," Air Force Cambridge Research Lab., AFCRL 66-412, No. 3, Bedford, MA, May 1966, p. 54.
- <sup>4</sup>Ramo, S., Whinnery, J. R., and Van Duzer, T., *Electromagnetic Fields and Waves in Communication Electronics*, 2nd ed., Wiley, New York, 1984, pp. 191-193.
- <sup>5</sup>Jensen, M. D., "Investigation of Accuracy Limitations of the Ionospheric Plasma Frequency Probe and Recommendations for a New Instrument," M.S. Thesis, Utah State Univ., Logan, UT, May 1988.
- <sup>6</sup>Jensen, M. D., and Howlett, L. C., "Wide Frequency Range Sinewave VCO with a Tuneable Inductor and Capacitor," *IEEE Transactions on Instrumentation and Measurement*, Vol. 38, No. 4, 1989, pp. 876-881.
- <sup>7</sup>Swenson, C. M., "An Evaluation of the Plasma Frequency Probe," M.S. Thesis, Utah State Univ., Logan, UT, 1989.
- <sup>8</sup>Poularikas, A. D., and Seely, S., *Signals and Systems*, PWS-Kent, Boston, MA, 1985, pp. 370-383.
- <sup>9</sup>Swenson, C. M., Kelly, M. C., Primdahl, F., and Baker, K. D., "CRIT II Electric, Magnetic, and Density Measurements Within an Ionizing Neutral Stream," *Geophysical Research Letters*, Vol. 17, No. 12, 1990, pp. 2337-2340.

Alfred L. Vampola  
Associate Editor